Communications in Numerical Analysis 2016 No.2 (2016) 92-107

Available online at www.ispacs.com/cna
Volume 2016, Issue 2, Year 2016 Article ID cna-00233, 16 Pages
doi:10.5899/2016/cna-00233
Research Article

Thermal Radiation Effects on Squeezing Flow Casson Fluid between Parallel Disks

Sheikh Irfanullah Khan[1, 2], Umar Khan[2], Naveed Ahmed[2], Syed Tauseef Mohyud-Din[2*]

(1) COMSATS Institute of Information Technology, University Road, Abbottabad, Pakistan
(2) Department of Mathematics, Faculty of Sciences, HITEC University, Taxila Cantt, Pakistan

Abstract
In this paper, we investigate the thermal radiation effects in a time-dependent two-dimensional flow of a Casson fluid between two parallel disks when upper disk is taken to be impermeable and lower one is porous. Suitable similarity transforms are employed to convert governing partial differential equations into system of ordinary differential equations. Well known Homotopy Analysis Method (HAM) is employed to obtain the expressions for velocity and temperature profiles. Effects of different physical parameters such as squeeze number *S*, Prandtl number *Pr*, Eckert number *Ec* and the dimensionless length on the flow are also discussed with the help of graphs for velocity and temperature coupled with a comprehensive discussions. The skin friction coefficient and local Nusselt number along with convergence of the series solutions obtained by HAM are presented in tabulated form, while numerical solution is obtained by RK-4 method and comparison shows an excellent agreement between both the solutions.

Keywords: Homotopy analysis method (HAM); Casson fluid; radiation effect; squeezing flow; parallel disks; numerical solution.

1 Introduction

Squeezing flow between parallel disks is an important area of interest because of its application in bio fluid mechanics like pumping of heart, flow through certain arteries, polymer industry process, injection modeling, compression, liquid-metal lubrication, and the squeezed films in power transmission. Most frequently, squeezing flows were illustrated in modeling of metal and plastic sheets, thin fiber and paper sheets formations etc. After the pioneer work done by Stefan (1874) [1], several attempts are reported that extended the traditional problem to heat transfer case. Different studies are available in literature that used various solution schemes to get analytical and numerical solutions for the said problem. Siddiqui et al. [2] examined two-dimensional MHD squeezing flow between parallel plates. For parallel disk similar problem

* Corresponding Author. Email address: syedtauseefs@hotmail.com, Tel: +92 3235577701

has been discussed by Domairry and Aziz [3]. Both used Homotopy perturbation method (HPM) to determine the solution. Some studies related to channel flows can be found in [4-14]

Joneidi et al. [15] studied the mass transfer effect on squeezing flow between parallel disks using Homotopy analysis method (HAM). Most recently influence of heat transfer in the MHD squeezing Flow between parallel disks has been investigated by T. Hayat et al. [16]. They used HAM to solve the resulting nonlinear system of ordinary differential equations. Since then squeezing flow has been of great interests for various researchers [17-19].

Investigations with heat transport phenomenon are important in many industrial applications such as wire coating, hot rolling, metal spinning, glass blowing, paper manufacturing, glass fiber, glass sheet productions, the drawing of plastic films, continuous casting and the aerodynamic extrusion of plastic sheets. Radiative heat transfer plays an important role in controlling where convective heat transfer coefficients are small. In polymer industry, the radiative heat transfer is an essential phenomenon for the design of reliable equipment's, nuclear plants, gas turbines, etc. The process of radiative heat transfer is also important in free and forced convection flows. Keeping all these applications in mind, many authors studied various research problems for the case of radiative heat transfer. Some of these can be seen in [20-23] and references there in.

High nonlinearity of governing equations in various flow problems means unlikeliness of exact solution. To cope up with these problems, many approximation techniques have been developed. Highly nonlinear problems such as the ones discussed above are therefore solved by using these techniques. These include, Adomian's Decomposition Method (ADM), Variational Iteration Method, Variation of Parameters Method, Homotopy Perturbation Method, Homotopy Analysis Method, etc. [24-31].

Mathematical models describing the realistic flow problems mostly involve the Non-Newtonian fluids. One of these fluids is known as Casson fluid and its formulation is provided in [32-33] is found to suitable for blood flow problems up to large extent.

Casson fluid flow between squeezing disks under radiative heat transfer has not been considered yet. To fill out this gap, heat transfer analysis for squeezing flow of Casson fluid between parallel disks under the effects of thermal radiation is presented. Well known Homotopy Analysis Method (HAM) [34-41] Numerical solution is also sought to check the validity of analytical solution. A detailed comparison between purely analytical solution obtained by HAM and the numerical solution obtained employing R-K 4 method is presented. Graphs are plotted to analyze the effects of different emerging parameters on velocity and temperature profiles.

2 Mathematical Analysis

We have investigated parallel infinite disks *h* distance apart with magnetic field practiced vertically and is proportional to $B_0\left(1-at\right)^{1/2}$. Incompressible Casson fluid is used in between the disks. Magnetic field is negligible for low Reynold numbers. Consequently, Casson fluid flow equation is delineated as [42-45]

$$\tau_{ij}=\begin{Bmatrix} 2\left[\mu_B+\left(\frac{p_y}{2\pi}\right)\right]e_{ij}, & \pi>\pi_c \\ 2\left[\mu_B+\left(\frac{p_y}{2\pi_c}\right)\right]e_{ij}, & \pi_c>\pi \end{Bmatrix}$$

where p_y is yield stress of fluid, μ_B the plastic-dynamic viscosity of the fluid and π is the self-product of component of deformation rate with itself and π_c is the critical value of the said self-product.

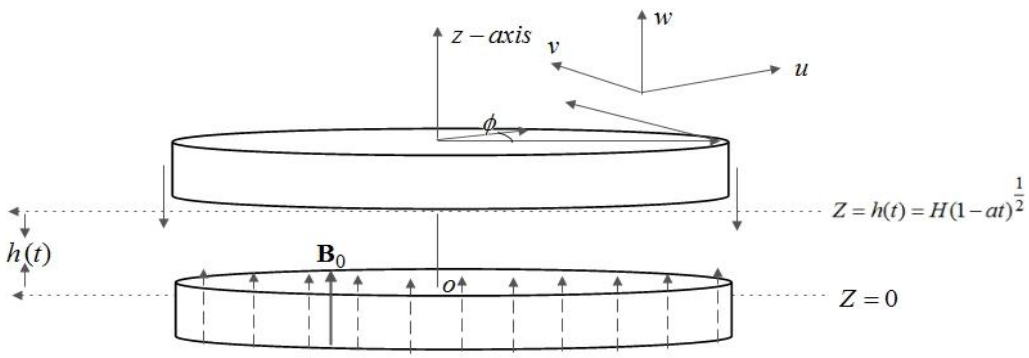

Figure 1: Schematics diagram of the problem

The physical configuration of the problem is presented in Figure 1. T_w and T_h are constant temperatures lower d upper disk respectively. The viscous dissipation effects in the energy equation are retained. We have chosen the cylindrical coordinates system $(r,\ \emptyset,\ z)$ where the upper disk is moving with velocity $\frac{aH(1-at)^{-1/2}}{2}$ towards or away from the stationary lower disk. Thus, the constitutive equations for two-dimensional flow and heat transfer of a viscous fluid under the effects of thermal radiation can be written as:

$$\frac{\partial \bar{u}}{\partial r}+\frac{\bar{u}}{r}+\frac{\partial \bar{w}}{\partial z}=0 \tag{2.1}$$

$$\rho\left(\frac{\partial \bar{u}}{\partial t}+\bar{u}\frac{\partial \bar{u}}{\partial r}+\bar{w}\frac{\partial \bar{u}}{\partial z}\right)=-\frac{\partial \hat{p}}{\partial r}+\mu\left(\frac{1+\beta}{\beta}\right)\left(\frac{\partial^2 \bar{u}}{\partial r^2}+\frac{1}{r}\frac{\partial \bar{u}}{\partial r}-\frac{\bar{u}}{r^2}+\frac{\partial^2 \bar{u}}{\partial z^2}\right)-\frac{\sigma}{\rho}B^2(t)\bar{u}, \tag{2.2}$$

$$\rho\left(\frac{\partial \bar{w}}{\partial t}+\bar{u}\frac{\partial \bar{w}}{\partial r}+\bar{w}\frac{\partial \bar{w}}{\partial z}\right)=-\frac{\partial \hat{p}}{\partial z}+\mu\left(\frac{1+\beta}{\beta}\right)\left(\frac{\partial^2 \bar{w}}{\partial r^2}+\frac{\partial^2 \bar{w}}{\partial z^2}+\frac{1}{r}\frac{\partial \bar{w}}{\partial r}\right), \tag{2.3}$$

$$C_p\left(\frac{\partial T}{\partial t}+\bar{u}\frac{\partial T}{\partial r}+\bar{w}\frac{\partial T}{\partial z}\right)=\frac{K_0}{\rho}\left(\frac{\partial^2 T}{\partial r^2}+\frac{\partial^2 T}{\partial z^2}+\frac{1}{r}\frac{\partial T}{\partial r}-\frac{\bar{u}}{r^2}\right)+\frac{16\sigma^* T_H^3}{3k^*}\frac{\partial^2 T}{\partial z^2}. \tag{2.4}$$

With side conditions

$$\left\{\bar{u}=0,\ \bar{w}=-w_0\right\}\Big|_{z=0}$$
$$\left\{\bar{u}=0,\ \bar{w}=\frac{dh}{dt}\right\}\Big|_{z=h(t)} \tag{2.5}$$

$$T=T_0\big|_{z=0}$$
$$T=\frac{2T_0-atT_0}{1-at}\Big|_{z=h(t)} \tag{2.6}$$

In the above equations $\bar{u}$ and $\bar{w}$ are the velocity components in the *r*- and *z* - directions respectively, while ρ is the density, viscosity μ, $\hat{p}$ the pressure, specific heat C_p, *T* the temperature, *v* kinematic viscosity, K_0 thermal conductivity, k^* mean absorption coefficient, Stefan Boltzmann constant σ^*, and w_0 is suction/injection velocity.

Substituting the following transformations [46]

$$\bar{u}=\frac{ar}{2(1-at)}\bar{F}'(\eta),\quad \bar{w}=-\frac{aH}{\sqrt{1-at}}\bar{F}(\eta),$$
$$B(t)=\frac{B_0}{\sqrt{1-at}},\quad \eta=\frac{z}{H\sqrt{1-at}},\quad \theta(\eta)=\frac{(T-T_0)(1-at)}{T_0}, \tag{2.7}$$

in Eqs. (2.2) - (2.4) and removing the pressure gradient from the subsequent equations, we finally obtain

$$\left(1+\frac{1}{\beta}\right)\overline{F}^{(iv)} - S\left(\eta\overline{F}''' + 3\overline{F}'' - 2\overline{F}\,\overline{F}'''\right) - M^2\widetilde{F}'' = 0, \tag{2.8}$$

$$\left(1+\frac{4}{3}R_d\right)\overline{\theta}'' + S\,\mathrm{Pr}\left(2\overline{F}\,\overline{\theta}' - \eta\overline{\theta}'\right) + \left(1+\frac{1}{\beta}\right)\mathrm{Pr}\,Ec\left(\overline{F}''^2 + 12\delta^2\overline{F}'^2\right) = 0, \tag{2.9}$$

with associated condition

$$\begin{aligned} &\overline{F}(0) = A, \quad \overline{F}'(0) = 0, \quad \theta(0) = 1, \\ &\overline{F}(1) = \tfrac{1}{2}, \quad \overline{F}'(1) = 0, \quad \theta(1) = 0. \end{aligned} \tag{2.10}$$

Where A denotes the suction/injection, Eckert number Ec, Hartman number M, squeeze number S, Prandtl number Pr, radiation parameter R_d, and δ the dimensionless length defined as

$$\begin{aligned} &S = \frac{aH^2}{2\nu},\ M^2 = \frac{aB_0^2H^2}{\nu},\ \mathrm{Pr} = \frac{\mu C_p}{K_0},\ R_d = \frac{4\sigma^*T_\infty^3}{k^*k}, \\ &Ec = \frac{1}{C_p(T_w - T_h)}\left(\frac{ar}{2(1-at)}\right)^2,\ \delta^2 = \frac{H^2(1-at)}{r^2}. \end{aligned} \tag{2.11}$$

The skin friction coefficient and Nusselt number are defined as

$$C_{fr} = \frac{\tau_{rz}\big|_{z=h(t)}}{\rho\left(\frac{-aH}{2(1-at)}\right)^2}, \quad Nu = \frac{Hq_w}{K_0(T_w - T_h)}, \tag{2.12}$$

where

$$\tau_{rz} = \mu\left(\frac{\partial u}{\partial z} + \frac{\partial w}{\partial r}\right)\Bigg|_{z=h(t)}, \quad q_w = -k_0\left(\frac{\partial T}{\partial z}\right)\Bigg|_{z=h(t)}. \tag{2.13}$$

In view of (2.7), Eq. (2.12) can be written as

$$C_{fr} = \left(1+\frac{1}{\beta}\right)\frac{\overline{F}''(1)r^2}{H^2\,\mathrm{Re}_r}, \quad Nu = -\frac{\theta'(1)}{\sqrt{1-at}}, \tag{2.14}$$

$$\mathrm{Re}_r = \frac{raH(1-at)^{1/2}}{2\nu}. \tag{2.15}$$

3 Solution Procedure for HAM

Tracking the methodology proposed by Liao [34-35], we can initiate initial guesses as

$$F_0(\eta) = A + \frac{3}{2}(1+2A)\eta^2 + (-1+2A)\eta^3, \tag{3.16}$$

$$\theta_0(\eta) = \eta. \tag{3.17}$$

Linear operator can be chosen as

$$\overline{L}_F = \frac{d^4\overline{F}}{d\eta^4} \text{ and } \overline{L}_\theta = \frac{d^2\overline{\theta}}{d\eta^2} \tag{3.18}$$

Above operators satisfies the following linearity,

$$\bar{L}_F\left(C_1 + C_2\eta + C_3\eta^2 + C_4\eta^3\right) = 0, \tag{3.19}$$

$$\bar{L}_\theta\left(C_5 + C_6\eta\right) = 0, \tag{3.20}$$

Where $C_i\left(i = 1-6\right)$ are constants.

3.1. Zero-Order Deformation

Representing $\hat{p} \in [0,1]$ as the embedding parameter, zero-order problem can be formulated as

$$(1-\hat{p})\bar{L}_F[F(\eta,\hat{p}) - F_0(\eta)] = \hat{p}h_F\hat{N}_F[\bar{F}(\eta,\hat{p})], \tag{3.21}$$

$$\bar{F}(0,\hat{p}) = A;\ \bar{F}'(0,\hat{p}) = 0;\ \bar{F}(1,\hat{p}) = \frac{1}{2};\ \bar{F}'(1,\hat{p}) = 0, \tag{3.22}$$

$$(1-\hat{p})\bar{L}_\theta[\bar{\theta}(\eta,\hat{p}) - \theta_0(\eta)] = \hat{p}h_\theta\hat{N}_\theta[\bar{\theta}(\eta,\bar{p})], \tag{3.23}$$

$$\bar{\theta}(0,\hat{p}) = 1;\ \bar{\theta}(1,\hat{p}) = 0, \tag{3.24}$$

where, h_F, h_θ are nonzero auxiliary parameters.

Nonlinear operators are

$$\begin{aligned}
\hat{N}_F[\bar{F}(\eta,\hat{p})] &= \frac{\partial^4\bar{F}}{\partial\eta^4} + S\left(\frac{1}{1+\beta}\right)\left(\eta\frac{\partial^3\bar{F}}{\partial\eta^3} + 3\frac{\partial^2\bar{F}}{\partial\eta^2} - 2\bar{F}\frac{\partial^3\bar{F}}{\partial\eta^2}\right) - M^2\left(\frac{1}{1+\beta}\right)\frac{\partial^2\bar{F}}{\partial\eta^2},\\
\hat{N}_\theta[\bar{\theta}(\eta,\hat{p})] &= \frac{\partial^2\bar{\theta}}{\partial\eta^2} + S\,\mathrm{Pr}\left(\frac{3}{3+4R_d}\right)\left(2\bar{F}\frac{\partial\bar{\theta}}{\partial\eta} + \eta\frac{\partial\bar{\theta}}{\partial\eta}\right) + \mathrm{Pr}\,Ec\left(\frac{3}{3+4R_d}\right)\left(\frac{1+\beta}{\beta}\right)\left(\left(\frac{\partial^2\bar{F}}{\partial\eta^2}\right)^2 + 12\delta^2\left(\frac{\partial\bar{F}}{\partial\eta}\right)^2\right).
\end{aligned} \tag{3.25}$$

3.2. mth-Order Deformation Problem

The mth-order problems satisfy

$$\bar{L}_F\left[\bar{F}_m(\eta) - \chi_m\bar{F}_{m-1}(\eta)\right] = h_F\Re_m^F(\eta), \tag{3.26}$$

$$\bar{L}_\theta\left[\bar{\theta}_m(\eta) - \chi_m\bar{\theta}_{m-1}(\eta)\right] = h_\theta\Re_m^\theta(\eta), \tag{3.27}$$

$$\bar{F}_m(0) = \bar{F}_m'(0) = \bar{F}_m(1) = \bar{F}_m'(1) = 0, \tag{3.28}$$

$$\bar{\theta}_m(0) = \bar{\theta}_m(1) = 0. \tag{3.29}$$

Where

$$\begin{aligned}
\Re_m^F(\eta) &= \bar{F}_{m-1}^{(iv)}(\eta) + S\left(\frac{1}{1+\beta}\right)\left(\eta\bar{F}_{m-1}''' + 3\bar{F}_{m-1}''\right) - M^2\left(\frac{1}{1+\beta}\right)\bar{F}_{m-1}''\\
&\quad - 2S\left(\frac{1}{1+\beta}\right)\left(\sum_{k=0}^{m-1}\left(\bar{F}_{m-1-k}\bar{F}_k'''\right)\right),\\
\Re_m^\theta(\eta) &= \bar{\theta}_{m-1}''(\eta) - S\,\mathrm{Pr}\left(\frac{3}{3+4R_d}\right)\left(\eta\bar{\theta}_{m-1}'\right) + 2S\,\mathrm{Pr}\left(\sum_{k=0}^{m-1}\left(\bar{F}_{m-1-k}\bar{\theta}_k'\right)\right)\\
&\quad + \mathrm{Pr}\,Ec\left(\frac{3}{3+4R_d}\right)\left(1+\frac{1}{\beta}\right)\left(\sum_{k=0}^{m-1}\left(\bar{F}_{m-1-k}''\bar{F}_k'' - 12\delta^2\bar{F}_{m-1-k}'\bar{F}_k'\right)\right),
\end{aligned} \tag{3.30}$$

also

$$\chi = \begin{cases} 0, & m \le 1 \\ 1, & m > 1 \end{cases}. \tag{3.31}$$

For $\hat{p}=0$ and $\hat{p}=1$ we have

$$\bar{F}(\eta,0)=F_0(\eta), \quad \bar{F}(\eta,1)=\bar{F}(\eta), \tag{3.32}$$

$$\bar{\theta}(\eta,0)=\theta_0(\eta), \quad \bar{\theta}(\eta,1)=\theta(\eta). \tag{3.33}$$

Using Taylor's series in terms of *p* one can get

$$\bar{F}(\eta,\hat{p})=F_0(\eta)+\sum_{m=1}^{\infty}\bar{F}_m(\eta)\hat{p}^m, \qquad \bar{F}_m(\eta)=\frac{1}{m!}\frac{\partial^m\bar{F}(\eta,\hat{p})}{\partial\eta^m}\bigg|_{\hat{p}=0}, \tag{3.34}$$

$$\bar{\theta}(\eta,\hat{p})=\theta_0(\eta)+\sum_{m=1}^{\infty}\bar{\theta}_m(\eta)\hat{p}^m, \qquad \bar{\theta}_m(\eta)=\frac{1}{m!}\frac{\partial^m\bar{\theta}(\eta,\hat{p})}{\partial\eta^m}\bigg|_{\hat{p}=0}, \tag{3.35}$$

Substituting $\hat{p}=1$ in above equations we obtain

$$F(\eta)=F_0(\eta)+\sum_{m=1}^{\infty}\bar{F}_m(\eta), \tag{3.36}$$

$$\theta(\eta)=\theta_0(\eta)+\sum_{m=1}^{\infty}\bar{\theta}_m(\eta), \tag{3.37}$$

$\bar{F}_m(\eta)$ and $\bar{\theta}_m(\eta)$ can be obtained by solving set of Eqs. (3.26) - (3.29) using computer software Mathematica, while Eqs. (3.36) and (3.37) gives us the final solution.

3.3. Convergence of the Solution

As proposed by Liao [34-35] the auxiliary parameter *h* is the key to convergence of series solution, where acceptable range of this auxiliary parameter can be identified by the *h*-curves which is parallel to horizontal axis. Figure 2 is displayed to demonstrate convergence region for different auxiliary parameter at 16 th order of approximation. It clearly shows that the acceptable region of *h*-curves is to be between -1.8 and -0.2.

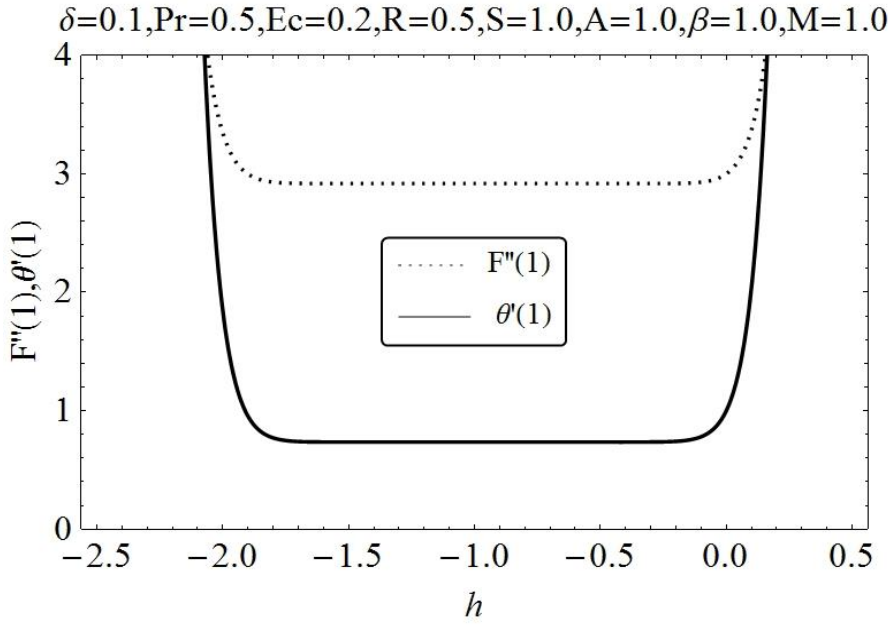

Figure 2: h curves for the function f and θ for different orders of approximations

4 Results and discussions

For convenience, we divide our discussions in to two parts one dedicated to investigate the upshots on varying physical parameter for the case suction ($A > 0$) and the other one describes the same effects for the case of blowing ($A < 0$).

Acceptable range for auxiliary parameter h has been discussed in previous section. In our analysis and discussions we use $h = -0.8$ as an optimal value of h for both velocity and temperature profiles. After ensuring the convergence of series solution our concern now is to see the influences of suction/blowing parameter, squeeze number *S* and Casson fluid parameter β on velocity and temperature profile is examined.

4.1. Suction Case

To analyze the impact of emerging parameters on velocity and temperature profile for suction, effects of squeezing parameter *S* on the velocity and temperature profile are discussed in Figures 3a & 3b. In Figure 3a velocity profile decreases in magnitude near the porous walls for $\eta \leq 0.4$ and the velocity profile decreases in magnitude for increasing value of squeeze numbers, while in Figure 3b temperature profile increases with increase in squeeze number *S*. Effect of Casson fluid parameter β for velocity and temperature profile is discussed in Figure 4a & 4b. In Figure 4a, increase in magnitude for velocity near the porous wall for Casson fluid parameter and decreases for increasing value of β, while temperature increases for increase in Casson fluid parameter.

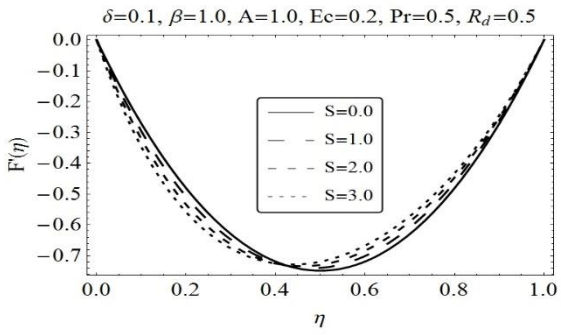

Figure 3: (a) Influence of S on $F'(\eta)$

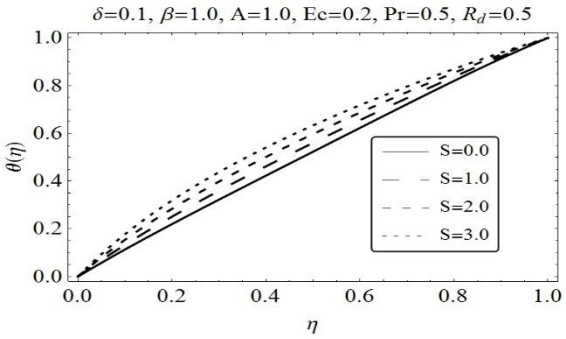

Figure 3: (b) Influence of S on $\theta(\eta)$

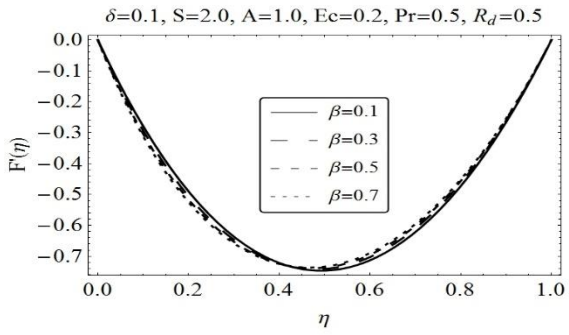

Figure 4: (a) Influence of $\boldsymbol{\beta}$ on $F'(\eta)$

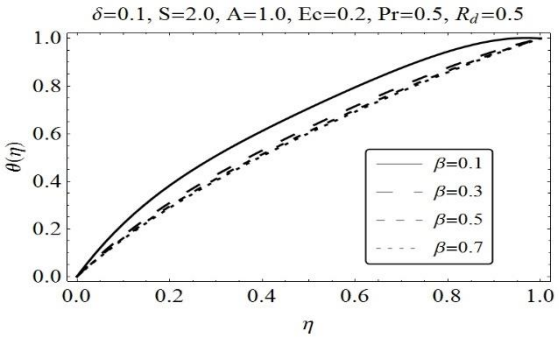

Figure 4: (b) Influence of $\boldsymbol{\beta}$ on $\theta(\eta)$

The graphical representations of key parameters in case of suction for temperature profile are displayed in Figures 5-8. Figure 5 depicts the influence of radiation parameter for suction case, increase in radiation parameter R_d results in increased temperature. Physically, increase in radiation parameter can give us higher values of temperature that can be used in many industrial appliances.

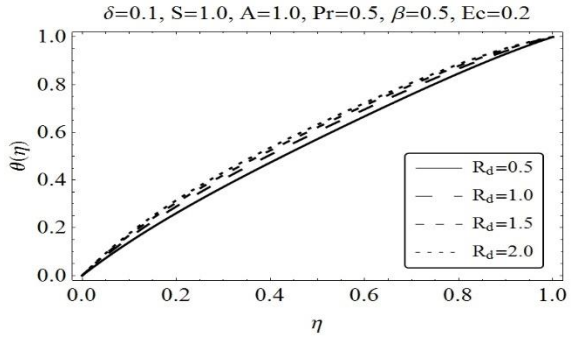

Figure 5: Influence of R_d on $\theta(\eta)$

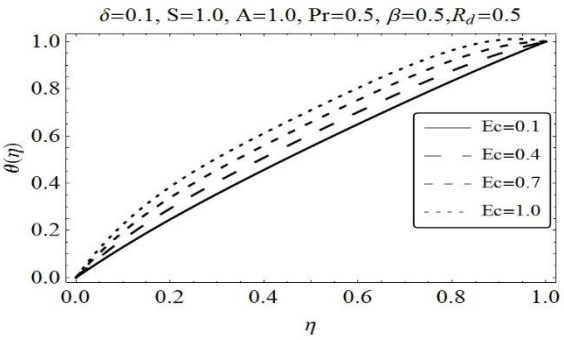

Figure 6: Influence of Ec on $\theta(\eta)$

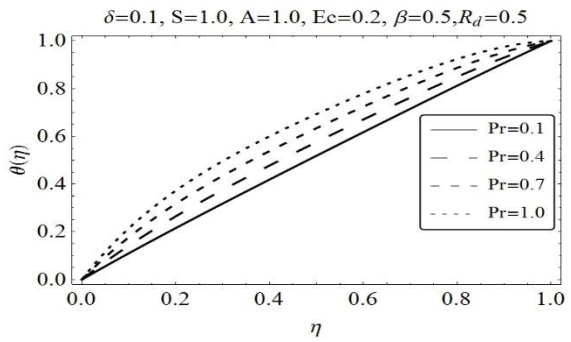

Figure 7: Influence of Pr on $\theta(\eta)$

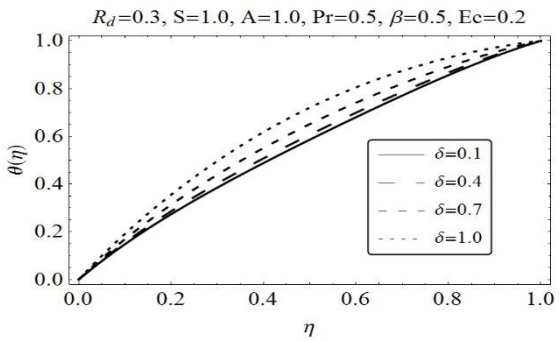

Figure 8: Influence of S on $\theta(\eta)$

Figure 6 depicts the behavior of *Ec* on the temperature distribution, where rapid rise in temperature is seen with higher *Ec*. However, for the higher *Ec* number boundary layer thickness decreases. This increase in temperature is due to the presence of viscous dissipation term in the energy equation. Figure 7 depicts the behavior of temperature for increasing values of Prandtl number. A rapid rise in temperature distribution is seen for the higher values of Pr, because of the fact that larger values of *Pr* have low thermal conductivity, which decreases the boundary layer thickness. The higher values of Prandtl numbers describes high viscosity oils and lower its thermal conductivity, while lighter values of *Pr* designates liquid-like material having low viscosity and increases the boundary layer thickness. The effect of dimensionless length δ is almost like Prandtl number that can be seen from Figure 7.

4.2. Blowing Case

To analyze the behavior of all emerging parameter on velocity and temperature profile for blowing case Figures 9-14 are displayed. It can be seems that the behavior of all physical parameter on velocity profile are opposite in blowing case as compared to those in suction case. Only difference is the effects of radiation parameter R_d that has opposite effects on temperature profile for suction and blowing cases.

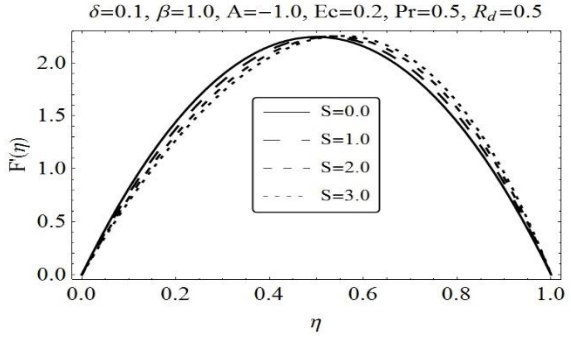

Figure 9: (a) Influence of S on $F'(\eta)$

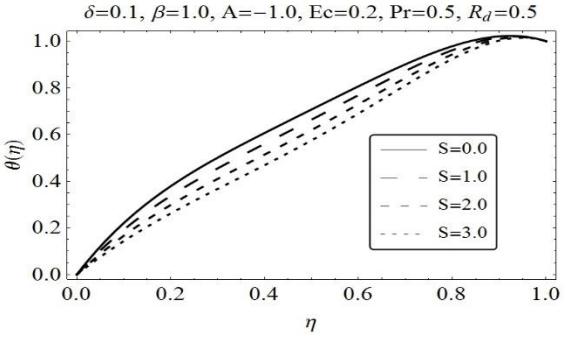

Figure 9: (b) Influence of S on $\theta(\eta)$

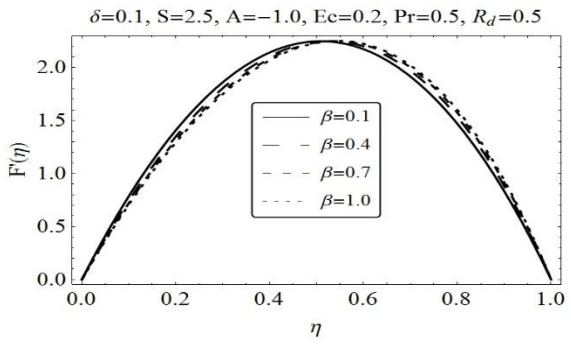

Figure 10: (a) Influence of $\boldsymbol{\beta}$ on $F'(\eta)$

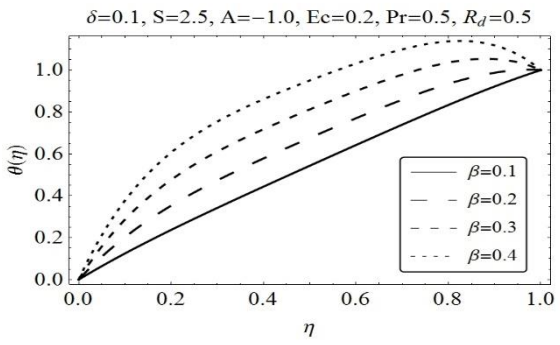

Figure 10: (b) Influence of $\boldsymbol{\beta}$ on $\theta(\eta)$

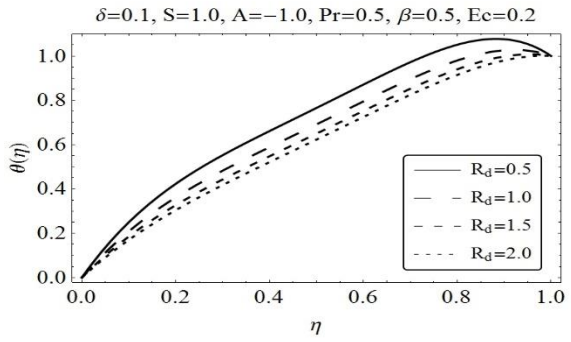

Figure 11: Influence of R_d on $\theta(\eta)$

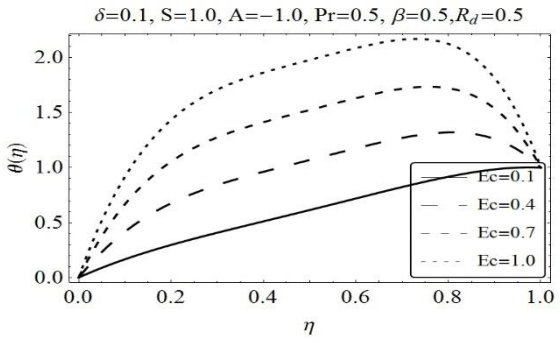

Figure 12: Influence of Ec on $\theta(\eta)$

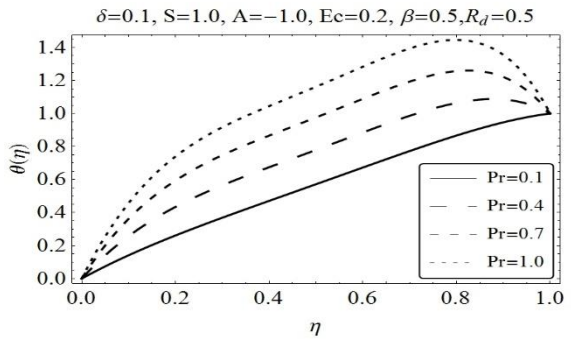

Figure 13: Influence of Pr on $\theta(\eta)$

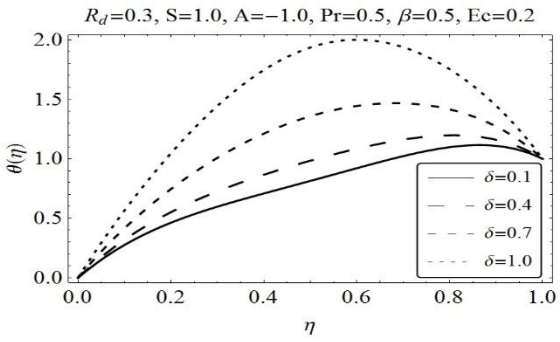

Figure 14: Influence of S on $\theta(\eta)$

Same problem is solved numerically by using Runge-Kutta method of order 4. Comparison of analytical and numerical result is presented in Table 1. It can be seems that both numerical and analytical solutions are in outstanding agreement.

Table 2 and 3 displayed the numerical value of skin friction coefficient and local Nusselt number for various physical parameters. It can be seems that, the magnitude of skin friction coefficient decreases with an increase in *A*.

Table 1: Comparison of HAM and numerical solution for $\delta = 0.1,\ A = 0.1 = S,\ R_d = 0.5$

	$F'(\eta)$		$\theta(\eta)$	
η	**HAM**	**Numerical**	**HAM**	**Numerical**
0	**1**	**1**	**0**	**0**
0.1	**0.984447**	**0.984447**	**0.163528**	**0.163528**
0.2	**0.943592**	**0.943592**	**0.293261**	**0.293261**
0.3	**0.885229**	**0.885229**	**0.405012**	**0.405012**
0.4	**0.816181**	**0.816181**	**0.507993**	**0.507993**
0.5	**0.742583**	**0.742583**	**0.606914**	**0.606914**
0.6	**0.670113**	**0.670113**	**0.703222**	**0.703222**
0.7	**0.604195**	**0.604195**	**0.795729**	**0.795729**
0.8	**0.550188**	**0.550188**	**0.795729**	**0.795729**
0.9	**0.513550**	**0.513550**	**0.952048**	**0.952048**
1	**0.5**	**0.5**	**1**	**1**

Table 2: Values of skin friction coefficient and the Nusselt number for different values of *A, S,* and R_d.

A	***S***	R_d	$\left(1+\frac{1}{\beta}\right)F''(1)$	***Pr***	***Ec***	δ	$\theta'(1)$
0.0	**0.1**	**0.5**	**-33.0635**	**0.5**	**0.2**	**0.1**	**-0.002158**
0.1			**-26.4479**				**0.357588**
0.2			**-19.8337**				**0.637159**
0.3			**-13.2210**				**0.836573**
0.1	**0.1**		**-26.4479**				**0.357588**
	0.2		**-26.4557**				**0.356379**
	0.3		**-26.4636**				**0.355171**
	0.4		**-26.4715**				**0.353964**
	0.1	**0.1**	**-26.4479**				**0.055355**
		0.2	**-26.4479**				**0.154768**
		0.3	**-26.4479**				**0.235250**
		0.4	**-26.4479**				**0.301737**

Table 3: Values of Nusselt number $(1-at)^{1/2}\,Nu$ for different values of *Pr, Ec,* and δ when $A = 0.1,\ S = 0.1,\ R_d = 0.5$

Pr	***Ec***	δ	$(1-at)^{1/2}\,Nu$
0.1			**0.8715**
0.2			**0.7430**
0.3			**0.6145**
0.4			**0.4860**
0.5	**0.0**		**0.9986**
	0.2		**0.3576**
	0.4		**-0.2834**
	0.6		**-0.9244**
	0.3	**0.0**	**-0.2364**
		0.5	**-1.0910**
		1.0	**-2.5153**
		2.0	**-4.5093**

5 Conclusion

This article studies the squeezing flow of a Casson fluid between parallel disks under the effects of thermal radiation. Governing equations are transformed to set of ordinary differential equations are solved using a well-known method, i.e., Homotopy Analysis Method (HAM). Effects of different emerging parameters on velocity and temperature profiles are discussed with the help of graphs. Numerical solution is also carried out to confirm the results obtained by HAM. It can be concluded that for the case of suction, velocity profile behaves quite oppositely as compared to the case of injection for all varying parameters. While the temperature profile has almost similar behavior for both the cases except the radiation parameter, it behaves oppositely for the case of suction and injection.

Acknowledgements

Authors would like to thank the anonymous reviewers for their valuable comments that really improved the quality of this article.

References

[1] M. J. Stefan, Versuch Über die scheinbare adhesion,Sitzungsberichte der Akademie der Wissenschaften in Wien, Mathematik-Naturwissen, 69 (1874) 713-721.

[2] A. M. Siddiqui, S. Irum, A. R. Ansari, Unsteady squeezing flow of a viscous MHD fluid between parallel plates, M. Mod. Ana, 13 (2008) 565-576.
http://dx.doi.org/10.3846/1392-6292.2008.13.565-576

[3] G. Domairy, A. Aziz, Approximate Approximate Analysis of MHD Squeeze Flow between Two Parallel Disks with Suction or Injection by Homotopy Perturbation Method, Mathematical Problems in Engineering, article ID/2009/603916.
http://dx.doi.org/10.1155/2009/603916

[4] A. J. Chamkha, Hydromagnetic Two-Phase Flow in a Channel, International Journal of Engineering Science, 33 (1995) 437-446.
http://dx.doi.org/10.1016/0020-7225(93)E0006-Q

[5] A. J. Chamkha, Solutions for Fluid-Particle Flow and Heat Transfer in a Porous Channel, International Journal of Engineering Science, 34 (1996) 1423-1439.
http://dx.doi.org/10.1016/0020-7225(96)00036-5

[6] A. J. Chamkha, Unsteady Flow of an Electrically Conducting Dusty-Gas in a Channel Due to an Oscillating Pressure Gradient, Applied Mathematical Modelling, 21 (1997) 287-292.
http://dx.doi.org/10.1016/S0307-904X(97)00018-8

[7] A. J. Chamkha, Unsteady Laminar Hydromagnetic Fluid-Particle Flow and Heat Transfer in Channels and Circular Pipes, International Journal of Heat and Fluid Flow, 21 (2000) 740-746.
http://dx.doi.org/10.1016/S0142-727X(00)00031-X

[8] A. J. Chamkha, Flow of Two-Immiscible Fluids in Porous and Non-Porous Channels, ASME Journal of Fluids Engineering, 122 (2000) 117-124.
http://dx.doi.org/10.1115/1.483233

[9] A. J. Chamkha, Unsteady Laminar Hydromagnetic Flow and Heat Transfer in Porous Channels with Temperature-Dependent Properties, International Journal of Numerical Methods for Heat & Fluid Flow, 11 (2001) 430-448.
http://dx.doi.org/10.1108/EUM0000000005529

[10] A. J. Chamkha, On Laminar Hy dromagnetic Mixed Convection Flow in a Vertical Channel with Symmetric and Asymmetric Wall Heating Conditions, International Journal of Heat and Mass Transfer, 44 (2002) 2509-2525.
http://dx.doi.org/10.1016/S0017-9310(01)00342-8

[11] A. J. Chamkha, T. Grosan and I. Pop, Fully Developed Free Convection of a Micropolar Fluid in a Vertical Channel, International Communications in Heat and Mass Transfer, 29 (2002) 1119-1127.
http://dx.doi.org/10.1016/S0735-1933(02)00440-2

[12] A. J. Chamkha, T. Grosan and I. Pop, Fully Developed Mixed Convection of a Micropolar Fluid in a Vertical Channel, International Journal of Fluid Mechanics Research, 30 (2003) 251-263.
http://dx.doi.org/10.1615/InterJFluidMechRes.v30.i3.10

[13] J. C. Umavathi, J. P. Kumar, A. J. Chamkha, I. Pop, Mixed Convection in a Vertical Porous Channel, Transport in Porous Media, 61 (2005) 315-335.
http://dx.doi.org/10.1007/s11242-005-0260-5

[14] J. P. Kumar, J. C. Umavathi, A. J. Chamkha, I. Pop, Fully Developed Free Convective Flow of Micropolar and Viscous fluids in a Vertical Channel, Applied Mathematical Modelling, 35 (2010) 1175-1186.
http://dx.doi.org/10.1016/j.apm.2009.08.007

[15] A. A. Joneidi, G. Domairry, M. Babaelahi, Effect of mass transfer on the flow in the magnetohydrodynamic squeeze film between two parallel disks with one porous disk, Chem. Eng. Comm., 198 (2011) 299-311.
http://dx.doi.org/10.1080/00986445.2010.512533

[16] T. Hayat, A. Yousuf, M. Mustafa, S. Asghar, Influence of Heat Transfer in the Squeezing Flow Between Parallel Disks, Chem. Eng. Comm, 199 (2012) 1044-1062.
http://dx.doi.org/10.1080/00986445.2011.631203

[17] U. Khan, N. Ahmed, S. I. U. Khan, Z. A. Zaidi, X. J. Yang, S. T. Mohyud-Din, On unsteady two-dimensional and axisymmetric squeezing flow between parallel plates, Alexandria Engineering Journal, 53 (2014) 463-468.
http://dx.doi.org/10.1016/j.aej.2014.02.002

[18] U. Khan, N. Ahmed, Z. A. Zaidi, M. Asadullah, S. T. Mohyud-Din, MHD Squeezing Flow between Two Infinite Plates, Ain Shams Engineering Journal, 5 (2014) 187-192.
http://dx.doi.org/10.1016/j.asej.2013.09.007

[19] S. I. U. Khan, U. Khan, N. Ahmed, S. U. Jan, S. T. Mohyud-Din, Heat transfer analysis for squeezing flow between parallel disks, Journal of the Egyptian Mathematical Society, (2015),
http://dx.doi.org/10.1016/j.joems.2014.06.011

[20] Y. Khan, Q. Wu N. Faraz, A. Yldrm, S. T. Mohyud-Din, Heat Transfer Analysis on the Magnetohydrodynamic Flow of a Non-Newtonian Fluid in the Presence of Thermal Radiation: An Analytic Solution, Zeitschrift für Naturforschung A, 67 (2012) 147-152.
http://dx.doi.org/10.5560/zna.2012-0001

[21] S. Nadeem, Rizwan Ul Haq, Effect of Thermal Radiation for Megnetohydrodynamic Boundary Layer Flow of a Nanofluid Past a Stretching Sheet with Convective Boundary Conditions, Journal of Computational and Theoretical Nanoscience, 11(2013) 32-40.
http://dx.doi.org/10.1166/jctn.2014.3313

[22] M. M. Rashidi, S. Abbasbandy, Analytic approximate solutions for heat transfer of a micropolar fluid through a porous medium with radiation, Communications in Nonlinear Science and Numerical Simulation, 16 (4) (2011) 1874-1889.
http://dx.doi.org/10.1016/j.cnsns.2010.08.016

[23] N. S. Akbar, S. Nadeem, R. U. Haq, Z. H. Khan, Radiation effects on MHD stagnation point flow of nanofluid towards a stretching surface with convective boundary condition, Chinese Journal of Aeronautics, 26 (6) (2013) 1389-1397.
http://dx.doi.org/10.1016/j.cja.2013.10.008

[24] S. Abbasbandy, Homotopy perturbation method for quadratic Riccati differential equation and comparison with Adomian's decomposition method, Applied Mathematics and Computation, 172 (1) (2006) 485-490.
http://dx.doi.org/10.1016/j.amc.2005.02.014

[25] S. Abbasbandy, Modified homotopy perturbation method for nonlinear equations and comparison with Adomian decomposition method, Applied Mathematics and Computation, 172 (1) (2006) 431-438.
http://dx.doi.org/10.1016/j.amc.2005.02.015

[26] S. Abbasbandy, Numerical solution of non-linear Klein-Gordon equations by variational iteration method, International Journal for Numerical Methods in Engineering, vol. 70 (7) (2007) 876-881.
http://dx.doi.org/10.1002/nme.1924

[27] S. T. Mohyud-Din, A. Yldrm, S. A. Sezer, Analytical Approach to a Slowly Deforming Channel Flow with Weak Permeability, Zeitschrift für Naturforschung A, A Journal of Physical Sciences, (2010) 1033-1038.
http://dx.doi.org/10.1515/zna-2010-1202

[28] M. A. Abdou, A. A. Soliman, Variational iteration method for solving Burger's and coupled Burger's equations, J. Comput. Appl. Math, 181 (2005) 245-251.
http://dx.doi.org/10.1016/j.cam.2004.11.032

[29] M. A. Noor, S. T. Mohyud-Din, Variational iteration technique for solving higher order boundary value problems, Appl. Math. Comp, 189 (2007) 1929-1942.
http://dx.doi.org/10.1016/j.amc.2006.12.071

[30] M. A. Noor, S. T. Mohyud-Din, A. Waheed, Variation of parameters method for solving fifth-order boundary value problems, Applied Mathematics and Information Sciences, 2 (2008) 135-141.

[31] U. Khan, N. Ahmed, Z. A. Zaidi, S. U. Jan, S. T. Mohyud-Din, On Jeffery-Hamel Flows, International Journal of Modern Mathematical Sciences, 7 (2013) 236-247.

[32] E. W. Mrill, A. M. Benis, E. R. Gilliland, T. K. Sherwood, E. W. Salzman, Pressure flow relations of human blood hollow fibers at low flow rates, Journal of Applied Physiology, 20 (1965) 954-967.

[33] D. A. McDonald, Blood Flows in Arteries, 2nd ed., Arnold, London (1974).

[34] S. J. Liao, Beyond perturbation: introduction to the Homotopy Analysis Method, CRC Press, Boca Raton, Chapman and Hall, (2003).
http://dx.doi.org/10.1201/9780203491164

[35] S. J. Liao, On the homotopy analysis method for nonlinear problems, Applied Mathematics and Computation, 147 (2004) 499-513.
http://dx.doi.org/10.1016/S0096-3003(02)00790-7

[36] S. Abbasbandy, The application of homotopy analysis method to solve a generalized Hirota-Satsuma coupled KdV equation, Physics Letters A, 36 (2007) 478-483.
http://dx.doi.org/10.1016/j.physleta.2006.09.105

[37] S. Abbasbandy, F. S. Zakaria, Soliton solutions for the fifth-order K-dV Equation with the homotopy analysis method, Nonlinear Dynamics, 51 (2008) 83-87.
http://dx.doi.org/10.1007/s11071-006-9193-y

[38] R. Ellahi, A Study on the Convergence of Series Solution of Non-Newtonian Third Grade Fluid with Variable Viscosity: By Means of Homotopy Analysis Method, Advances in Mathematical Physics, Article ID 634925, 2012 (2012) 11 pages.
http://dx.doi.org/10.1155/2012/634925

[39] R. Ellahi, The effects of MHD and temperature dependent viscosity on the flow of non-Newtonian nanofluid in a pipe: Analytical solutions, Applied Mathematical Modeling, 37 (2013) 1451-1467.
http://dx.doi.org/10.1016/j.apm.2012.04.004

[40] R. Ellahi, T. Hayat, F. M. Mahomed, A. Zeeshan, Analytical solutions for MHD flow in an annulus, Communications in Nonlinear Sciences and Numerical Simulation, 15 (2010) 1224-1227.
http://dx.doi.org/10.1016/j.cnsns.2009.05.050

[41] R. Ellahi, M. Raza, K. Vafai, Series solutions of non-Newtonian nanofluids with Reynolds' model and Vogel's model by means of the homotopy analysis method, Mathematical and Computer Modelling, 55 (2012) 1876-1891.
http://dx.doi.org/10.1016/j.mcm.2011.11.043

[42] S. Nadeem, R. U. Haq, C. Lee, MHD flow of a Casson fluid over an exponentially shrinking sheet, Scientia Iranica, 19 (2012) 1150-1553.
http://dx.doi.org/10.1016/j.scient.2012.10.021

[43] S. Nadeem, R. U. Haq, N. S. Akbar, Z. H. Khan, MHD three dimensional flow of Casson fluid past a porous linearly Stretching sheet, Alexandria Engineering Journal, 52 (2013) 577-582. *http://dx.doi.org/10.1016/j.aej.2013.08.005*

[44] N. Ahmed, U. Khan, X. J. Yang, S. I. U. Khan, Z. A. Zaidi, S. T. Mohyud-Din, Magneto hydrodynamic (MHD) squeezing flow of a Casson fluid between parallel disks, International Journal of Physical Sciences, 8 (36) (2013) 1788-1799.

[45] U. Khan, N. Ahmed, S. I. U. Khan, S. Bano, S. T. Mohyud-Din, Unsteady squeezing flow of a casson fluid between parallel plates, World Journal of Modelling and Simulation, 10 (4) (2014) 308-319.

[46] T. Hayat, A. Qayyum, F. Alsasdi, M. Awais, A. M. Dobaie, Thermal Radiation effects in squeezing flow of a Jeffery fluid, The European Physical journal Plus, 85 (2013) 128.